

The J-Domain of Hsp40 Couples ATP Hydrolysis to Substrate Capture in Hsp70[†]

Pernilla Wittung-Stafshede,[‡] Jesse Guidry,[‡] B. Erin Horne,[§] and Samuel J. Landry^{*,§}

Department of Biochemistry, Tulane University Health Sciences Center, New Orleans, Louisiana 70112,
and Department of Chemistry, Tulane University, New Orleans, Louisiana 70118

Received December 9, 2002; Revised Manuscript Received February 21, 2003

ABSTRACT: The *Escherichia coli* Hsp40 DnaJ uses its J-domain to target substrate polypeptides for binding to the Hsp70 DnaK, but the mechanism of J-domain function has been obscured by a substrate-like interaction between DnaJ and DnaK. ATP hydrolysis in DnaK is associated with a conformational change that captures the substrate, and both DnaJ and substrate can stimulate ATP hydrolysis. However, substrates cannot trigger capture by DnaK in the presence of ATP, and substrates stimulate a DnaK conformational change that is uncoupled from ATP hydrolysis. The role of the J-domain was examined using the fluorescent derivative of a fusion protein composed of the J-domain and a DnaK-binding peptide. In the absence of ATP, DnaK-binding affinity of the fusion protein is similar to that of the unfused peptide. However, in the presence of ATP, the affinity of the fusion protein is dramatically increased, which is opposite to the decrease in DnaK affinity typically exhibited by peptides. Binding of a fusion protein that contains a defective J-domain is insensitive to ATP. According to results from isothermal titration calorimetry, the J-domain binds to the DnaK ATPase domain with weak affinity ($K_D = 23 \mu\text{M}$ at 20 °C). The interaction is characterized by a positive enthalpy, small heat capacity change ($\Delta C_p = -33 \text{ kcal mol}^{-1}$), and increasing binding affinity for increasing temperatures in the physiological range. In conditions that support binding of the J-domain to the ATPase domain, the J-domain accelerates ATP hydrolysis and a simultaneous conformational change in DnaK that is associated with peptide capture. The defective J-domain is inactive, despite the fact that it binds to the DnaK ATPase domain with higher than wild-type affinity. The results are most consistent with an allosteric mechanism of J-domain action in which the J-domain couples ATP hydrolysis to peptide capture by accelerating ATP hydrolysis and delaying DnaK closure until ATP is hydrolyzed.

Members of the 70 kDa molecular chaperone (Hsp70)¹ family mediate folding, assembly, and transport of proteins (1, 2). In these various processes, Hsp70s selectively bind to partially unfolded or disordered regions of proteins in an activity cycle that is controlled by the binding and hydrolysis of ATP (3, 4). A 44 kDa N-terminal domain contains an ATPase activity (5), and a 23 kDa C-terminal domain binds peptides in an extended conformation (6, 7). The ATP-bound state of Hsp70 is characterized by weak peptide binding, with rapid rates of association and dissociation (8). ATP hydrolysis is associated with a conformational change that converts Hsp70 to tight peptide binding (9). Intrinsic tryptophan fluorescence has been used to monitor ATP-dependent conformational changes in Hsp70 (10, 11), but peptide binding was shown to promote a similar conformational

change at rates that far exceed the rates of ATP hydrolysis (12).

DnaK is a well-characterized member of the Hsp70 family in *Escherichia coli*, whose synthesis is upregulated during stress (13). Modulation of the activity of DnaK is provided in *E. coli* by the cochaperones DnaJ and GrpE, which affect specific steps of the ATPase cycle (14, 15). DnaJ increases the ATP hydrolysis rate, and GrpE increases the rate of ADP/ATP exchange. DnaJ also stabilizes DnaK–substrate complexes and promotes loading of substrates onto DnaK (16–18).

Members of the 40 kDa molecular chaperone (Hsp40) family are structurally more diverse than Hsp70s (19, 20). The paradigmatic Hsp40, DnaJ, has an N-terminal J-domain, followed by a disordered Gly/Phe-rich domain, Zn²⁺-binding domain, and additional C-terminal domains that are involved in substrate binding and dimerization. The J-domain is the most highly conserved and most strongly implicated in Hsp70 regulation. Mutations in J-domains of Sec63 (21) and SV40 T-antigen (22, 23) as well as in conventional Hsp40s such as DnaJ (24) disrupt interactions with the relevant Hsp70s. The J-domain binds with weak affinity to the ATPase domain of DnaK (25), but the C-terminal domains have also been implicated in interactions with Hsp70 (26–31).

The mechanism by which DnaJ facilitates substrate delivery to DnaK is complicated by a bipartite interaction with DnaK. The DnaK ATPase is activated synergistically

[†] We acknowledge the Tulane University Wall Fund for support.

^{*} To whom correspondence should be addressed: (504) 586-3990 (phone); (504) 584-2739 (fax); landry@tulane.edu (e-mail).

[‡] Department of Chemistry, Tulane University.

[§] Department of Biochemistry, Tulane University Health Sciences Center.

¹ Abbreviations: Hsp70, 70 kDa heat shock protein; Hsp40, 40 kDa heat shock protein; Jd, recombinant J-domain of *Escherichia coli* DnaJ; JdD35N, recombinant D35N mutant J-domain; Jdp5, recombinant protein composed of the J-domain and peptide p5; JdD35Np5, recombinant protein composed of the D35N mutant J-domain and peptide p5; Jdp5A, acrylodan-labeled Jdp5; JdD35Np5A, acrylodan-labeled JdD35Np5; Kase, recombinant ATPase domain of *E. coli* DnaK.

by the combination of a synthetic peptide with a recombinant J-domain (26), and binding of DnaK to immobilized DnaJ is blocked by mutations in either the ATPase domain or peptide-binding domain of DnaK (29, 32, 33). Evidence that the J-domain alone can stimulate ATP hydrolysis or substrate capture has been lacking. J-domain molecules truncated precisely at the end of the J-domain were reportedly inactive (26, 28). In contrast, J-domain molecules containing C-terminal extensions stimulated ATP hydrolysis and capture of the J-domain molecule or of a separate substrate molecule (16, 26, 28). Thus, the C-terminal extension seems to be essential for expression of J-domain function.

To study the effect of the J-domain on peptide capture by DnaK, we prepared a fusion protein (Jdp5) composed of the J-domain and peptide p5, CLLLSAPRR. The DnaK-binding properties of a fluorescent acrylodan-labeled p5 have been described (34–36). We also prepared a mutant fusion protein (JdD35Np5) that incorporates the D35N substitution, which renders DnaJ defective (32). D35 is in the conserved His-Pro-Asp (HPD) tripeptide, which lies in a flexible loop between the coiled helices II and III (37). The HPD-containing loop is implicated in J-domain conformational dynamics (38), and it is located at the edge of the DnaK-binding site on helix II (25).

Binding studies with acrylodan-labeled versions of the fusion proteins (Jdp5A and JdD35Np5A) revealed that Jdp5A mimicked a DnaJ–substrate complex in that it bound with high affinity to DnaK in the presence of ATP. JdD35Np5A binding was not sensitive to ATP. The kinetics of Jdp5A binding suggested that a conformational change in DnaK follows the initial association, and this was confirmed by monitoring the tryptophan fluorescence of DnaK during binding of Jdp5. In contrast, binding of JdD35Np5A occurred in a single kinetic phase, and JdD35Np5 did not induce the conformational change. The mechanism of J-domain action was studied using recombinant wild-type and mutant J-domains (Jd and JdD35N). Jd coordinately stimulates ATP hydrolysis and a conformational change in DnaK. JdD35N does not stimulate either process, despite its binding to the recombinant DnaK ATPase domain (Kase) with higher than wild-type affinity. Since the DnaK conformational change is associated with closing of the peptide-binding domain, these experiments reveal for the first time that the J-domain couples ATP hydrolysis to peptide capture.

MATERIALS AND METHODS

Proteins. The QuickChange site-directed mutagenesis kit (Stratagene) was used for modification of protein-coding sequences. Plasmids directing the expression of Jdp5 and JdD35Np5 were derivatives of pPLJ_{AK3} (kind gift of R. McMacken), which is equivalent to pRLM232 (26), except for inconsequential differences in noncoding sequences. Mutagenic oligonucleotides were used to insert the sequence encoding the p5 peptide (CLLLSAPRR) followed by a stop codon on the 3' side of codon 78 in the DnaJ-coding sequence. The resulting plasmid was used to construct the derivative encoding the D35N mutation using appropriate oligonucleotides. The plasmid directing expression of JdD35N was a derivative of pRLM233 (26). The expression and purification of Jd, JdD35N, Jdp5, and JdD35Np5 from *E. coli* Nap IV cells was as described by Karzai and McMacken

(26), except that glycerol was omitted from buffer solutions. Dithiothreitol also was omitted from buffers used for purification of Jd and JdD35N. DnaK and Kase (DnaK residues 2–388) were prepared from *E. coli* C600 cells containing pRLM163 and pRLM156, respectively (15). DnaK preparations were extensively dialyzed in buffer containing 25 mM HEPES–NaOH, pH 7, 50 mM KCl, 5 mM MgCl₂, and 5 mM β-mercaptoethanol to remove DnaK-bound nucleotide.

Protein Modification with Acrylodan. Jdp5 or JdD35Np5 was desalted to remove dithiothreitol in a pD10 column (Pharmacia) equilibrated with 100 mM sodium phosphate, pH 7.0. Acrylodan (Molecular Probes, 10 mM in dimethylformamide) was added dropwise over several minutes to the protein (1 mg mL^{−1}) in a vessel wrapped in foil, and then the mixture was left at 4 °C overnight. The mixture was centrifuged at 30000g for 20 min. Protein in the supernatant was separated from low-molecular-weight components and concentrated by ultrafiltration (CentriPrep-10, Amicon). According to the mass spectrum, the protein modified with a single acrylodan group was the predominant species. Protein concentration was determined by Bio-Rad protein assay, and the extent of derivatization (75–90%) was determined using the ϵ_{360} (12900 M^{−1} cm^{−1}) for the acrylodan moiety.

K_D Determinations. Fluorescence–titration experiments were carried out using a PTI Quantamaster with excitation and emission slit widths of 3 nm and the temperature in a 1 cm × 1 cm cell maintained at 25 °C with a circulating water bath. At each concentration of DnaK, fluorescence emission was scanned in 1 nm increments from 460 to 540 nm upon excitation at 370 nm. The increase in fluorescence emission upon binding to DnaK, ΔF , was the emission intensity at 490 nm (average of nine points centered at 490 nm) for the sample with DnaK minus the emission intensity for the sample without DnaK. To determine values of K_D , data for ΔF vs DnaK concentration were fitted to the equation $\Delta F = \Delta F_{\max}(PL/L_t) = [\Delta F_{\max}/2L_t][(K_D + L_t + P_t) - ((-K_D - L_t - P_t)^2 - (4L_tP_t))^{1/2}]$, where L_t is the total concentration of Jdp5A or JdD35Np5A, P_t is the total concentration of DnaK, and PL is the concentration of a protein–DnaK complex. Additional methods are in the figure legends.

DnaK-Binding Kinetics in the Presence of ATP. An Applied PhotoPhysics SX18.MV stopped-flow spectrofluorometer was used to monitor rapid changes in acrylodan emission associated with Jdp5A or JdD35Np5A. The excitation wavelength was 370 nm, and the emission was monitored at 500 nm for 2 s. Both excitation and emission slit widths were set to 2.5 nm.

DnaK-Binding Kinetics in the Absence of ATP. A Cary Eclipse spectrofluorometer was used to monitor acrylodan emission associated with Jdp5A or JdD35Np5A. The excitation wavelength was set to 370 nm, and the emission was monitored at 500 nm for 20–60 min. The slit widths for both the excitation and emission were set to 5 nm. The average time for each point taken was 3 s. Data recorded after the first minute describe the pseudo-first-order rate of association with DnaK and thus were fitted to a single-exponential function.

Calorimetry. Proteins were dialyzed together into 50 mM morpholinoethanesulfonic acid (MOPS)–NaOH, pH 6.7, and chilled samples were degassed under house vacuum prior to

being loaded into the VP-ITC (MicroCal). Jd or JdD35N (1.15 mM) was titrated into Kase (initially, 0.048 mM). The reference power was set to $10 \mu\text{cal s}^{-1}$. Baseline heats of dilution determined by injecting Jd or JdD35N into buffer were not appropriate for subtraction from actual experiments with Kase. Instead, the baseline heat of dilution was treated as a variable in fitting each curve of ΔH vs protein ratio.

Single-Turnover ATPase Activity of DnaK. Single-turnover ATPase rates were measured at 20°C essentially as described by Russell et al. (15). Briefly, reaction mixtures described in the legend for Figure 3 were incubated for 5 min. Immediately, and at specific time points, $8 \mu\text{L}$ samples were combined with $2 \mu\text{L}$ of 1 N HCl. Subsequently, $2 \mu\text{L}$ from each time point was spotted onto poly(ethylenimine)–cellulose thin-layer chromatography sheets and developed in 1 M formic acid and 0.5 M lithium chloride. After completely dried, images of the radioactivity were recorded on Fuji PhosphorImaging plates and analyzed on a Fuji BAS 3000. The quantity of $[\alpha\text{-}^{32}\text{P}]\text{ADP}$ at each time point was corrected for the background level present in samples lacking DnaK, and then the progress of ADP production was fitted to a double-exponential function.

Stimulation of DnaK Conformational Change. For experiments with Jd or JdD35N, a Cary Eclipse spectrofluorometer was used to monitor DnaK tryptophan fluorescence at 20°C . The excitation wavelength was set to 293 nm, and the emission was monitored at 350 nm. The slit widths for both the excitation and emission were 2.5 nm. The average time for each point was 3 s. Within 1 min after addition of ATP, Jd or JdD35N was added, and the recording continued for 2 h. Data recorded after 4 min were normalized to span the range of 0–1 and fitted to a single-exponential function. For experiments with Jdp5 or JdD35Np5, an Applied Photo-Physics SX18.MV stopped-flow spectrofluorometer was used to monitor rapid changes in DnaK tryptophan emission. The excitation wavelength was 293 nm, and the emission was monitored at 350 nm. Both excitation and emission slit widths were set to 2.5 nm.

RESULTS

DnaK Affinity of Jdp5A and JdD35Np5A. Binding of Jdp5A and JdD35Np5A to DnaK was monitored by the increase in fluorescence of the acrylodan moiety, as described by Christen and co-workers for acrylodan-modified peptides (8). Upon binding to DnaK, the fluorescence intensity increased 2-fold, and the wavelength maximum shifted 15 nm toward the blue. These fluorescence changes are virtually identical to those observed for the p5A peptide (34), suggesting that the p5A portion of the fusion proteins engaged the peptide-binding domain of DnaK in the same manner (Figure 1A,B, insets). A similar binding experiment with a recombinant DnaK molecule that lacks the peptide-binding domain produced no change in the acrylodan fluorescence, demonstrating that the fluorescence change reports an interaction with the peptide-binding domain (data not shown).

In the presence of ATP, the affinity of Jdp5A was more than 100-fold higher than in the absence of ATP (Figure 1A, Table 1). This result contrasts with the nearly 100-fold reduction in affinity of p5A in the presence of ATP. The affinity of JdD35Np5A increased less than 2-fold in the

presence of ATP (Figure 1B). Thus, fusion to the wild-type J-domain enhanced the DnaK affinity of the peptide in the presence of ATP by more than 10000-fold.

In the absence of ATP, the affinities of Jdp5A and JdD35Np5A for DnaK were similar to each other and similar to the affinity of p5A. The data for acrylodan fluorescence change were fit with quadratic functions, but the data for Jdp5A in the absence of ATP are sigmoidal. The fit of Jdp5A binding vs $\log [\text{DnaK}]$ with the Hill equation yielded the midpoint reported in Table 1 and a Hill coefficient of 2.0 (not shown). The sigmoidal binding curve indicates that Jdp5A has two or more interacting sites that bind DnaK. We do not have a satisfactory explanation for the sigmoidal curve, but it is likely to involve both the peptide and the J-domain in Jdp5A. The hyperbolic curve for JdD35Np5A suggests that a sigmoidal curve requires a functional interaction between the J-domain and DnaK. Furthermore, in the absence of ATP, DnaK is known to form dimers that dissociate to monomers upon binding to a substrate polypeptide (39).

DnaK-Binding Kinetics of Jdp5A and JdD35Np5A. Rapid binding kinetics were monitored by acrylodan fluorescence after stopped-flow mixing. The fluorescence change in Jdp5A was best fit by a double exponential, whereas that for JdD35N was adequately fit by a single exponential (Figure 1, Table 1). Approximately 50% of the fluorescence change in Jdp5A and JdD35Np5A occurred in the dead time of the instrument, and thus it was not possible to measure the second-order DnaK association rates (k_{on}). Exceptionally fast association could be characteristic of p5-related sequences. Association of a-Ala-p5 (ALLLSAPRR with acrylodan coupled to the amino terminus) was found to have multiple phases, including at least one that was faster than could be measured (40). To estimate lower limits for k_{on} , the observed rates for $1 \mu\text{M}$ DnaK (fast phase for Jdp5A) were divided by the DnaK concentration. The slow phase of Jdp5A fluorescence change could not be fit reliably enough to determine whether it depended on DnaK concentration, and thus the rate observed at $1 \mu\text{M}$ DnaK is reported in Table 1. Experiments at lower Jdp5A and JdD35Np5A concentrations yielded similar rate constants, but the noise was greater, and the rates and amplitudes of the fast process were fit less consistently.

Binding of Jdp5A and JdD35Np5A to DnaK without ATP was slow, like that of p5A (Figure 1D, Table 1).

Thermodynamics of Jd and JdD35N Binding to Kase. In previous studies, the interaction of the J-domain with DnaK has been found to be weak or not observed at all (25, 26, 28, 29, 32). Binding of Jd and JdD35N to Kase was analyzed by isothermal titration calorimetry. Initial peaks associated with injection of Jd into Kase were positive, and therefore, binding is endothermic at this temperature (Figure 2). In the course of the titration, peaks decreased until reaching nearly the level observed for injection of Jd into buffer lacking Kase, indicating that the binding was near saturation.

The observed ΔH corresponds to a heat that is comparable in magnitude to the background heat of mixing the Jd solution with buffer alone. Thus, the precision of ΔH depends on an appropriate estimate of the background heat of mixing. The heat observed upon injection of Jd into buffer ($0.24 \text{ kcal mol}^{-1}$) was significantly larger than the value approached at high Jd:Kase ratio ($0.17\text{--}0.20 \text{ kcal mol}^{-1}$). Thus, for each

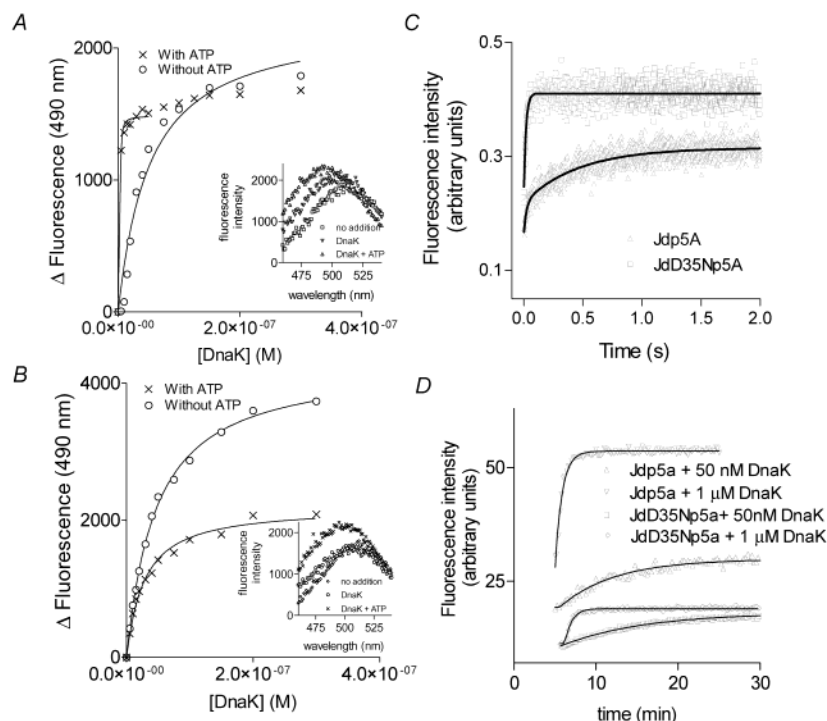


FIGURE 1: Binding of DnaK to Jdp5A and JdD35Np5A in the presence and absence of ATP. (A, B) DnaK was titrated into samples of 5 nM Jdp5A (A) or JdD35Np5A (B), 50 mM HEPES–NaOH, pH 7.6, 10 mM KCl, 1 mM MgCl₂, and, where indicated, 0.5 mM ATP. Binding to DnaK (20 nM) causes an increase in fluorescence intensity of acrylodan (insets). ATP dramatically enhances the DnaK-binding affinity of Jdp5A, as indicated by the shift of the curve to lower DnaK concentrations. (C) Binding kinetics in the presence of 2 mM ATP and otherwise the same buffer as above were monitored by acrylodan emission following rapid mixing of equal volumes ($\sim 65 \mu\text{L}$) of Jdp5A or JdD35Np5A (final concentration, 0.2 μM) and DnaK (final concentration, 1–4 μM). The average of eight measurements was fitted to a single exponential for JdD35Np5A and double exponential for Jdp5A. Lower limits on the second-order rate constants were estimated from the illustrated fits and reported in Table 1. (D) Reactions in the absence of ATP were initiated by addition of DnaK (0.05–1 μM) to samples of Jdp5A or JdD35Np5A (5 nM) while monitoring the steady-state acrylodan emission. The kinetics of association with DnaK conform to single exponentials and are similar for Jdp5A and JdD35Np5A. Second-order rate constants are reported in Table 1.

Table 1: DnaK-Binding Properties of J-Domain-Containing Fusion Proteins and Constituent Domains

ligand	K_D (μM)			k_{on} ($\text{M}^{-1} \text{s}^{-1}$) (+ATP)	k_{off} (s^{-1})		k_{on} ($\text{M}^{-1} \text{s}^{-1}$) (–ATP)	k_{off} (s^{-1})
	+ATP	–ATP						
Jdp5A	0.00022 ^a	0.03 ^b	binding	$> 45 \times 10^6$	0.01 ^c		4.9×10^4	0.0029 ^c
JdD35Np5A	0.024 ^a	0.04	binding	$> 54 \times 10^6$	1.2 ^c		3.2×10^4	0.0013 ^c
p5A	5 ^d	0.05 ^d		1.1×10^6 ^d	5.7 ^d	binding	2×10^4 ^d	0.0010 ^d
Jd		20 ^e					0.004 s^{-1d}	
JdD35N		4.7 ^e						

^a Apparent K_D determined by titration with DnaK and monitored by acrylodan fluorescence (Figure 1). ^b Concentration of half-maximal binding from the fit to the Hill equation (see text). ^c Derived from K_D and k_{on} . ^d From refs 36 and 48. ^e From calorimetry at 20 °C with Kase (Figure 2).

experiment, the heat of mixing the two protein solutions was estimated by sampling the quality of fit (X^2) with a range of values in increments corresponding to 0.01 kcal mol^{–1}. In all cases, a clear optimum was obtained. The fitting error in ΔH reported by the software algorithm (Microcal Origin) was larger than the increments in heat of mixing, and thus the fitting error was adopted for the overall error in ΔH for a particular experiment. However, the global uncertainty in measurements from multiple experiments was larger, presumably due to variations in solution composition and pH. The global uncertainty was estimated with a series of experiments in which Jd and Kase were dialyzed together on three separate occasions. The average and standard deviations of fitted values for the three experiments were as follows: $N = 1.14 \pm 0.35$, $K_A = 43500 \pm 6400 \text{ M}^{-1}$ (corresponding to $K_D = 23 \mu\text{M}$ and range 20.0–27.0 μM),

and $\Delta H = 0.41 \pm 0.25 \text{ kcal mol}^{-1}$. The K_D for Jd binding to Kase is similar to the previous estimate from NMR studies (25).

In a calorimetry experiment in which Jd and JdD35N were dialyzed together with Kase, the fitted values for JdD35N were as follows: $N = 1.04$, $K_A = 213000 \pm 28000 \text{ M}^{-1}$ (corresponding to $K_D = 4.69 \mu\text{M}$ and range 5.39–4.14 μM), and $\Delta H = 0.49 \pm 0.02 \text{ kcal mol}^{-1}$. The difference in K_D for JdD35N and Jd was larger than the experimental error and larger than the global uncertainty; thus, JdD35N binds to Kase with higher affinity than Jd.

The enthalpy of Jd binding to Kase progressively decreased at 20, 30, and 40 °C (Table 2). ΔC_p for T in the physiological range was obtained from the plot of ΔH vs T , which was well fit by a line with slope $-33 \pm 1 \text{ cal mol}^{-1} \text{ K}$.

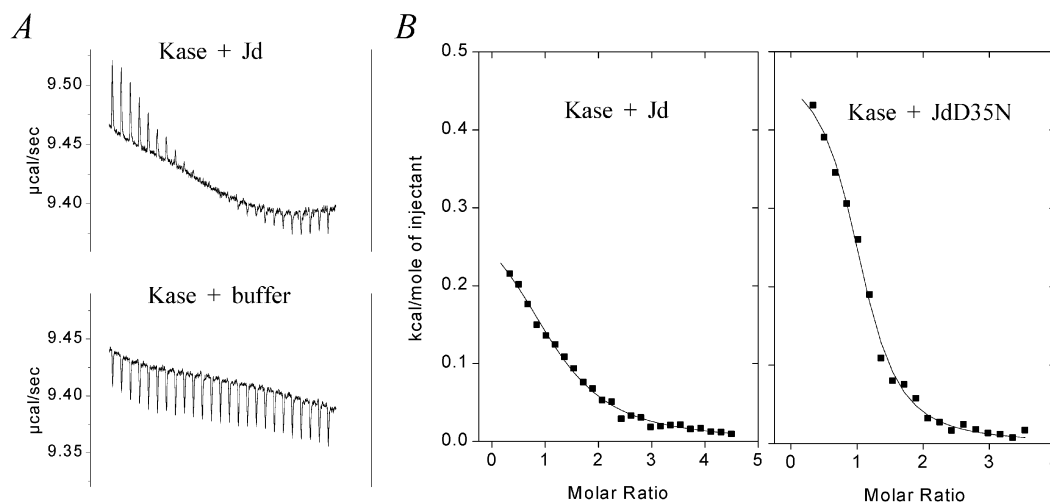


FIGURE 2: Isothermal titration calorimetry of Jd and JdD35N binding to Kase at 20 °C. (A) Raw calorimetry traces during injections of Jd and buffer alone to a solution of Kase. (B) Thermodynamics were analyzed by fitting ΔH vs molar ratio of Jd:Kase or JdD35N:Kase. Optimal fits were obtained with Kase-binding stoichiometries of 1.2 for Jd and 1.0 for JdD35N, suggesting that they form 1:1 complexes.

Table 2: Temperature Dependence of Jd Binding to Kase

	20 °C	30 °C	40 °C
N	0.77	1.15	1.30
$K_A \times 10^{-3} \text{ (M}^{-1}\text{)}$	40.5 ± 7.8	72.2 ± 14	132 ± 43
$K_D \text{ (}\mu\text{M)}$	20.7–30.6	11.6–17.2	5.7–11.2
$\Delta H \text{ (kcal)}$	0.70 ± 0.14	0.38 ± 0.03	0.038 ± 0.004
$\Delta G \text{ (kcal)}$	−6.18	−6.74	−7.33
$\Delta S \text{ (cal K}^{-1}\text{)}$	23.1	23.1	23.2

Stimulation by Jd of ATP Hydrolysis in DnaK. The ability of Jd and JdD35N to stimulate $[\alpha\text{-}^{32}\text{P}]\text{ATP}$ hydrolysis by DnaK was tested under single-turnover conditions as described (15). In some experiments, the hydrolysis was biphasic. The faster phase may be explained by the presence of contaminants with ATPase activity. The presence of contaminating ATPase in preparations of DnaK has been reported (15). Thus, we confine our interpretation here to the slower phase, which had the typical rate for DnaK. Without stimulants, ATP hydrolysis proceeded slowly, with a rate constant of 0.016 min^{-1} . In contrast to the previous report (26), Jd alone stimulated DnaK ATPase activity, and the degree of stimulation depended on Jd concentration (Figure 3, inset). JdD35N did not stimulate the DnaK ATPase activity at any concentration tested.

Stimulation by Jd and Jdp5 of a Conformational Change in DnaK. Previous studies have shown that DnaK's tryptophan emission reports on the state of the bound nucleotide and the conformation of the peptide-binding domain (10, 11). The ATP-bound open state has low fluorescence intensity, and the ADP-bound closed state has high fluorescence intensity. After binding ATP, DnaK gradually recovers the high fluorescence intensity on the time scale of 1–2 h (in parallel with ATP hydrolysis). However, peptides promote the conformational change in seconds (12). Since this is much faster than peptide-stimulated ATP hydrolysis, peptide binding uncouples the conformational change from ATP hydrolysis.

Here, we found that Jd accelerated the conformational change (Figure 3A), but the rate coincided with the rate of ATP hydrolysis (Figure 3B). Thus, Jd stimulated ATP hydrolysis and the conformational change in DnaK simultaneously. JdD35N did not stimulate the conformational

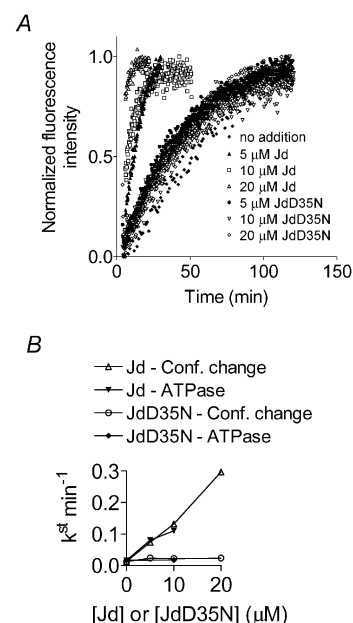


FIGURE 3: Stimulation of the DnaK conformational change and ATP hydrolysis by Jd but not JdD35N. (A) Tryptophan emission was monitored after reactions were initiated by addition of ATP (final concentration, $2 \mu\text{M}$) to a solution of 25 mM HEPES–NaOH, pH 7, 50 mM KCl, 5 mM MgCl_2 , 5 mM β -mercaptoethanol, $2 \mu\text{M}$ DnaK, and Jd or JdD35N at 20 °C. (B) Rates of the conformational change and ATP hydrolysis vs Jd or JdD35N concentration. ATPase assays were initiated by addition of radiolabeled ATP (final concentration, 2 nM cold ATP and 1 nM 3000 Ci/mmol $[\gamma\text{-}^{32}\text{P}]\text{-ATP}$) to a solution as above. Jd stimulates fluorescence recovery and ATP hydrolysis by DnaK to equal extents in a concentration-dependent manner.

change, which is consistent with its failure to stimulate ATP hydrolysis.

Results showing that Jd stimulates the DnaK ATPase activity are in apparent conflict with the study by McMacken and co-workers (26). However, that study employed a buffer system with much higher ionic strength, notably containing 0.3 M potassium glutamate. Indeed, we did not observe acceleration of the DnaK conformational change in that buffer system (data not shown). These results are consistent with the expectation that binding of the J-domain to the DnaK ATPase is dominated by electrostatic interactions.

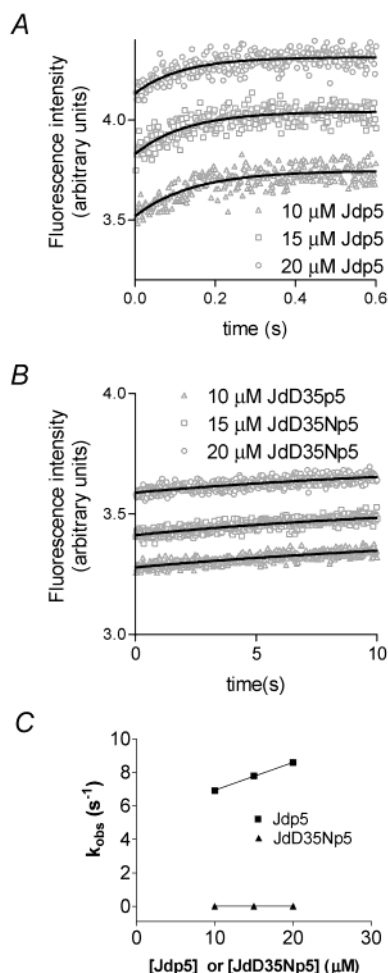


FIGURE 4: Stimulation of a rapid DnaK conformational change by Jdp5A but not JdD35Np5. (A, B) Binding-induced DnaK conformational changes in 25 mM HEPES–NaOH, pH 7.6, 50 mM KCl, 5 mM MgCl₂, and 5 mM β -mercaptoethanol monitored by tryptophan emission after rapid mixing of equal volumes ($\sim 65 \mu\text{L}$) of Jdp5 (A) or JdD35Np5 (B) and DnaK preloaded with 1 equiv of ATP. Concentrations of Jdp5 or JdD35Np5 are indicated in the symbol keys, and the concentration of DnaK was 1 μM . The average of 10 measurements was fitted to a single exponential. (C) Rates of conformational change vs Jdp5 or JdD35Np5 concentration. The rate constant for Jdp5 increased with DnaK concentration and was more than 1000 times faster than for JdD35Np5.

Stimulation by Jdp5 and JdD35Np5 of the DnaK conformational change was investigated by monitoring the recovery of tryptophan fluorescence after stopped-flow mixing in the presence of 1 equiv of ATP (Figure 4). Jdp5 stimulated a rapid recovery of tryptophan fluorescence in DnaK. A single exponential adequately described the recovery, and the rate constant depended on the concentration of Jdp5. At 10 μM Jdp5, the observed rate was 7.24 s⁻¹, or 27000-fold greater than the unstimulated rate. The apparent second-order rate constant was $1.7 \times 10^5 \text{ M}^{-1} \text{ s}^{-1}$. JdD35Np5 stimulated a much slower rate of recovery, and the rate was not sensitive to JdD35Np5 concentration over the range tested. At 10 μM JdD35Np5, the observed rate was 0.0058 s⁻¹, or 22-fold greater than the unstimulated rate.

DISCUSSION

The Jdp5A fusion protein mimicked a DnaJ–substrate complex in that it bound tightly to DnaK in the presence of ATP. The present observations support a mechanism in

which the J-domain, through appropriate J-domain–ATPase-domain interactions, couples ATP hydrolysis to capture of the peptide by DnaK. (i) The affinity of Jdp5A for DnaK was significantly greater than that of p5A only when ATP was present. (ii) Jd stimulated ATP hydrolysis and the conformational change in DnaK *simultaneously*. (iii) JdD35N failed to stimulate either ATP hydrolysis or the conformational change, despite the fact that it binds to the DnaK ATPase domain with higher than wild-type affinity. (iv) Biphasic DnaK association kinetics of Jdp5A suggested a capture step that follows association in the presence of ATP. Accordingly, DnaK association kinetics of JdD35Np5A lacked the second phase. (v) Jdp5 induced a rapid conformational change in DnaK that is associated with closing of the peptide-binding domain, whereas JdD35Np5 induced a conformational change on a much slower time scale.

A working model illustrates how the J-domain could couple the closure of the DnaK peptide-binding domain with ATP hydrolysis (Figure 5). Witt and co-workers have shown that peptide can stimulate closure of DnaK•ATP at rates that far exceed the rate of ATP hydrolysis. The Cro peptide (400 μM , 35 °C) stimulates the conformational change to a rate of 32 s⁻¹ but ATP hydrolysis to only 0.00067 s⁻¹ (12). Also, compare stimulation by p5 (10 μM , 25 °C) of the conformational change to 11 s⁻¹ (35) and ATP hydrolysis to 0.003 s⁻¹ (data not shown). Moreover, the closed state of DnaK is transient prior to ATP hydrolysis since the rate constant for reopening the p5•DnaK•ATP complex is 7.6 s⁻¹ (35). Thus, when DnaK is bound to both ligands (peptide and ATP), it has the fluorescence signature of the closed conformation, but the peptide-binding affinity is actually low because DnaK rapidly reopens prior to hydrolysis of ATP. The J-domain can reduce the peptide dissociation rate by almost 3 orders of magnitude by accelerating the rate of ATP hydrolysis and locking-in the peptide. The estimated dissociation rate for Jdp5A matches the rate of ADP/ATP exchange, 0.007 s⁻¹ (15), suggesting that Jdp5A dissociates from DnaK after ATP hydrolysis and upon binding of a new molecule of ATP.

An important issue is whether the J-domain can stimulate hydrolysis enough to capture the peptide before it dissociates. McMacken and co-workers have shown that DnaJ can stimulate ATP hydrolysis in DnaK by as much as 15000-fold (41). If applied to the basal ATPase rate at 25 °C, the stimulated rate would be 5 s⁻¹, which is comparable to the rate at which DnaK reopens to allow p5 dissociation.

The acrylodan fluorescence of Jdp5A and the tryptophan fluorescence of DnaK report kinetic phases of Jdp5A/Jdp5–DnaK binding that correspond to one or more conformational changes in DnaK. It is not clear that they report the same conformational change. We could not establish whether the second-order rate constants were the same nor even if the rate of the Jdp5A fluorescence change depended on DnaK concentration. Nevertheless, the absence of these kinetic phases for JdD35Np5A and JdD35Np5 provides compelling evidence that the conformational changes are related to each other and functionally significant. Moreover, the mutant J-domain reveals a potentially crucial aspect of J-domain function. Since the unfused p5 peptide can induce a rapid DnaK conformational change (35), the failure of JdD35Np5 to induce the rapid conformational change indicates that the mutant J-domain *blocks* the DnaK conformational change.

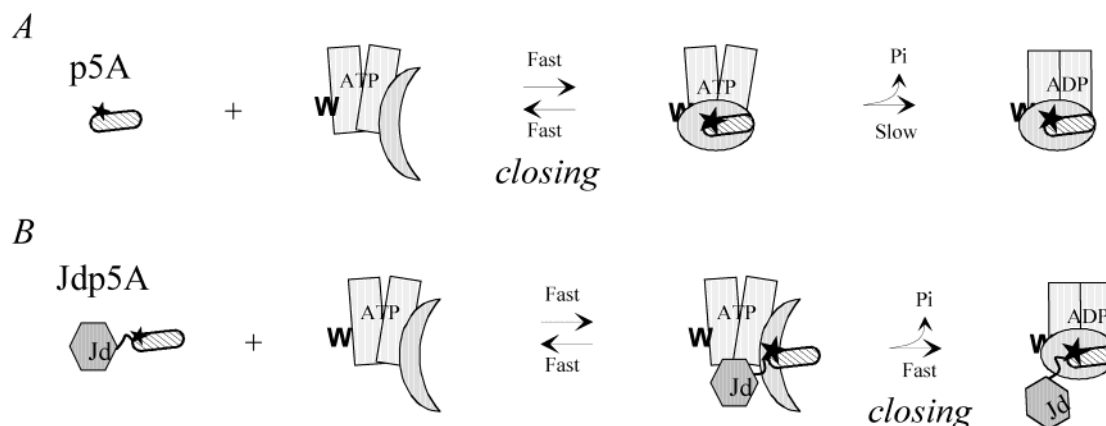
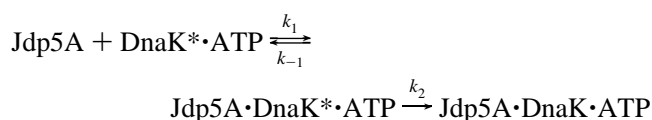


FIGURE 5: Model for J-domain function. The DnaK conformational change and ATP hydrolysis are uncoupled during binding of p5A (A) but coupled during binding of Jdp5A (B). The conformational change is illustrated as closure of the peptide-binding domain, which coincides with an increase in tryptophan fluorescence intensity. When p5A binds to DnaK, reopening of the peptide-binding domain is readily reversed prior to ATP hydrolysis, and thus the affinity is low. J-domain binding blocks closure of the peptide-binding domain until ATP is hydrolyzed.

The apparent second-order rate constant for the Jdp5-induced DnaK conformational change can be interpreted using a kinetic scheme proposed by Russell et al. for DnaJ-stimulated ATP hydrolysis (41). A rapid equilibrium precedes a rate-limiting conformational change:



Russell et al. indicated ADP·P_i in the complex after the conformational change characterized by k_2 . Here, we indicate ATP because we have monitored the conformational change directly and have not established whether ATP hydrolysis can be resolved as a separate kinetic step. Using the notation of Witt and co-workers, DnaK* denotes the ATP-bound "open" conformation of DnaK that has low tryptophan fluorescence (35). When $k_{-1} \gg k_2$, the apparent second-order rate constant corresponds to $k_1 k_2 / k_{-1}$ or k_2 / K_D , where K_D is the equilibrium dissociation constant for Jdp5A binding to DnaK·ATP. The K_D for Jdp5A binding to DnaK·ATP is unknown, but we assume that it could be no greater than the K_D measured for p5A, and thus, an upper limit for k_2 would be 0.9 s⁻¹. For comparison, Russell et al. estimated a value of 5 s⁻¹ on the basis of DnaJ-stimulated ATP hydrolysis by DnaK (41). Thus, the J-domain in Jdp5 appears to catalyze the rate-limiting conformational change in DnaK at a rate comparable to that achieved by the J-domain in DnaJ.

By stabilizing alternate DnaK conformations, the peptide and J-domain engage a mechanism that couples ATP hydrolysis with peptide capture. The nearly identical affinities of Jdp5A and p5A for DnaK in the absence of ATP suggest that the peptide-binding domain blocks access of the J-domain to its binding site on DnaK. Results with JdD35Np5A and JdD35Np5 in the presence of ATP suggest that the reverse is also true. The J-domain can block p5-induced closing of DnaK·ATP until ATP is hydrolyzed. Since the wild-type J-domain stimulates ATP hydrolysis, this block is rapidly removed, and the outcome is coupling of ATP hydrolysis with peptide capture.

The interdependence of the J-domain and substrate for binding to DnaK revealed in this work is consistent with

the proposal by McMacken and co-workers that DnaJ confers substrate specificity to DnaK by regulating the DnaK ATPase (41). Moreover, it provides a mechanism for that model by showing that the J-domain couples ATP hydrolysis to a conformational change in DnaK that captures the substrate. This work also establishes the mechanistic basis for earlier studies showing that the J-domain catalytically activates DnaK to bind substrates (16, 42), and it distinguishes the contribution of the J-domain from the contribution of C-terminal domains of DnaJ that also interact with DnaK (28, 29).

Endothermic protein–ligand complexes, such as that of Jd–Kase, typically are dominated by an electrostatic contribution to binding (43–45). Moreover, Jd–Kase binding resembles nonspecific DNA binding, which is characterized by a small heat capacity and a $\Delta S / \Delta G$ that is near the value predicted by theory for ion hydration (44). This is consistent with a binding interface that involves the basic surface of helix II on the J-domain (25) and the acidic groove on Kase (32, 33).

The small heat capacity also suggests that Jd and Kase bind to each other without a significant protein-folding transition (46). Since the NMR and crystallographic studies have indicated little structural disorder in Jd or Kase, their binding must be similar to that of rigid bodies although a conformational change from one folded state to another cannot be ruled out. Indeed, NMR perturbation studies suggest that the J-domain undergoes an induced fit conformational change when it binds to the DnaK ATPase domain (49). Electrostatic forces have been said to orient ligand binding in numerous protein systems (47). Such a mechanism could provide geometric constraint to the DnaJ–DnaK interaction while minimally impeding the kinetics of their association and dissociation.

The small ΔC_p of Jd–Kase binding contributes to the observed increase in binding affinity at elevated temperature. As a consequence, the J-domain's influence on substrate delivery to DnaK is expected to increase over the physiological temperature range, possibly allowing the DnaJ–DnaK chaperone system to be more discriminating as the load of non-native protein increases.

ACKNOWLEDGMENT

Thanks to N. K. Steede for technical assistance, the McMacken laboratory for plasmid clones, the Witt and Georgopoulos laboratories for results prior to publication, and the Bukau laboratory and the New Orleans Protein Folding Intergroup for discussion.

REFERENCES

- Mayer, M. P., and Bukau, B. (1998) *Biol. Chem.* 379, 261–268.
- Kelley, W. L. (1998) *Trends Biochem. Sci.* 23, 222–227.
- Flynn, G. C., Chappell, T. G., and Rothman, J. E. (1989) *Science* 245, 385–390.
- Lewis, M. J., and Pelham, H. R. B. (1985) *EMBO J.* 4, 3137–3143.
- Flaherty, K. M., Deluca-Flaherty, C., and McKay, D. B. (1990) *Nature* 346, 623–628.
- Landry, S. J., Jordan, R., McMacken, R., and Gierasch, L. M. (1992) *Nature* 355, 455–457.
- Zhu, X. T., Zhao, X., Burkholder, W. F., Gragerov, A., Ogata, C. M., Gottesman, M. E., and Hendrickson, W. A. (1996) *Science* 272, 1606–1614.
- Schmid, D., Baici, A., Gehring, H., and Christen, P. (1994) *Science* 263, 971–973.
- Liberek, K., Skowrya, D., Zylicz, M., Johnson, C., and Georgopoulos, C. (1991) *J. Biol. Chem.* 266, 14491–14496.
- Palleros, D. R., Reid, K. L., Shi, L., Welch, W. J., and Fink, A. L. (1993) *Nature* 365, 664–666.
- Farr, C. D., Slepnev, S. V., and Witt, S. N. (1998) *J. Biol. Chem.* 273, 9744–9748.
- Slepnev, S. V., and Witt, S. N. (1998) *Biochemistry* 37, 16749–16756.
- Tilly, K., Spence, J., and Georgopoulos, C. (1989) *J. Bacteriol.* 171, 1585–1589.
- Liberek, K., Marszalek, J., Ang, D., Georgopoulos, C., and Zylicz, M. (1991) *Proc. Natl. Acad. Sci. U.S.A.* 88, 2874–2878.
- Russell, R., Jordan, R., and McMacken, R. (1998) *Biochemistry* 37, 596–607.
- Liberek, K., Wall, D., and Georgopoulos, C. (1995) *Proc. Natl. Acad. Sci. U.S.A.* 92, 6224–6228.
- Gamer, J., Bujard, H., and Bukau, B. (1992) *Cell* 69, 833–842.
- Langer, T., Lu, C., Echols, H., Flanagan, J., Hayer, M. K., and Hartl, F. U. (1992) *Nature* 356, 683–689.
- Bork, P., Sander, C., Valencia, A., and Bukau, B. (1992) *Trends Biochem. Sci.* 17, 129.
- Cheetham, M. E., and Caplan, A. J. (1998) *Cell Stress Chaperones* 3, 28–36.
- Scidmore, M. A., Okamura, H. H., and Rose, M. D. (1993) *Mol. Biol. Cell* 4, 1145–1159.
- Sawai, E. T., Rasmussen, G., and Butel, J. S. (1994) *Virus Res.* 31, 367–378.
- Sullivan, C. S., Gilbert, S. P., and Pipas, J. M. (2001) *J. Virol.* 75, 1601–1610.
- Wall, D., Zylicz, M., and Georgopoulos, C. (1994) *J. Biol. Chem.* 269, 5446–5451.
- Greene, M. K., Maskos, K., and Landry, S. J. (1998) *Proc. Natl. Acad. Sci. U.S.A.* 95, 6108–6113.
- Karzai, A. W., and McMacken, R. (1996) *J. Biol. Chem.* 271, 11236–11246.
- Misselwitz, E., Staack, O., Matlack, K. E. S., and Rapoport, T. A. (1999) *J. Biol. Chem.* 274, 20110–20115.
- Suh, W. C., Lu, C. Z., and Gross, C. A. (1999) *J. Biol. Chem.* 274, 30534–30539.
- Mayer, M. P., Laufen, T., Paal, K., McCarty, J. S., and Bukau, B. (1999) *J. Mol. Biol.* 289, 1131–1144.
- Yan, W., and Craig, E. A. (1999) *Mol. Cell. Biol.* 19, 7751–7758.
- Sha, B., Lee, S., and Cyr, D. M. (2000) *Struct. Folding Des.* 8, 799–807.
- Suh, W. C., Burkholder, W. F., Lu, C. Z., Zhao, X., Gottesman, M. E., and Gross, C. A. (1998) *Proc. Natl. Acad. Sci. U.S.A.* 95, 15223–15228.
- Gassler, C. S., Buchberger, A., Laufen, T., Mayer, M. P., Schroder, H., Valencia, A., and Bukau, B. (1998) *Proc. Natl. Acad. Sci. U.S.A.* 95, 15229–15234.
- Gisler, S. M., Pierpaoli, E. V., and Christen, P. (1998) *J. Mol. Biol.* 279, 833–840.
- Slepnev, S. V., and Witt, S. N. (2002) *Biochemistry* 41, 12224–12235.
- Pierpaoli, E. V., Gisler, S. M., and Christen, P. (1998) *Biochemistry* 37, 16741–16748.
- Szyperski, T., Pellicchia, M., Wall, D., Georgopoulos, C., and Wuthrich, K. (1994) *Proc. Natl. Acad. Sci. U.S.A.* 91, 11343–11347.
- Huang, K., Ghose, R., Flanagan, J. M., and Prestegard, J. H. (1999) *Biochemistry* 38, 10567–10577.
- Palleros, D. R., Reid, K. L., McCarty, J. S., Walker, G. C., and Fink, A. L. (1992) *J. Biol. Chem.* 267, 5279–5285.
- Koller, M. F., Baici, A., Huber, M., and Christen, P. (2002) *FEBS Lett.* 520, 25–29.
- Russell, R., Karzai, A. W., Mehl, A. F., and McMacken, R. (1999) *Biochemistry* 38, 4165–4176.
- Misselwitz, B., Staack, O., and Rapoport, T. A. (1998) *Mol. Cell* 2, 593–603.
- Bradshaw, J. M., Mitaxov, V., and Waksman, G. (1999) *J. Mol. Biol.* 293, 971–985.
- Takeda, Y., Ross, P. D., and Mudd, C. P. (1992) *Proc. Natl. Acad. Sci. U.S.A.* 89, 8180–8184.
- Aoki, K., Taguchi, H., Shindo, Y., Yoshida, M., Ogasahara, K., Yutani, K., and Tanaka, N. (1997) *J. Biol. Chem.* 272, 32158–32162.
- Spolar, R. S., and Record, M. T. (1994) *Science* 263, 777–784.
- Wade, R. C., Gabdoulline, R. R., Ludemann, S. K., and Lounnas, V. (1998) *Proc. Natl. Acad. Sci. U.S.A.* 95, 5942–5949.
- Pierpaoli, E. V., Sandmeier, E., Baici, A., Schonfeld, H. J., Gisler, S., and Christen, P. (1997) *J. Mol. Biol.* 269, 757–768.
- Landry, S. J. (2003) *Biochemistry* 42, XXXX–XXXX.

BI0273330